Electronic Supplementary Material (ESI) for Dalton Transactions.

Synthesis, Structure and Properties of $[Co(NCS)_2(4\text{-}(4\text{-Chloro-benzyl})pyridine)_2]_n$, that shows Slow Magnetic Relaxations and a Metamagnetic Transition

Julia Werner, Zbigniew Tomkowicz, Michał Rams, Stefan G. Ebbinghaus, Tristan Neumann and Christian Näther

Content

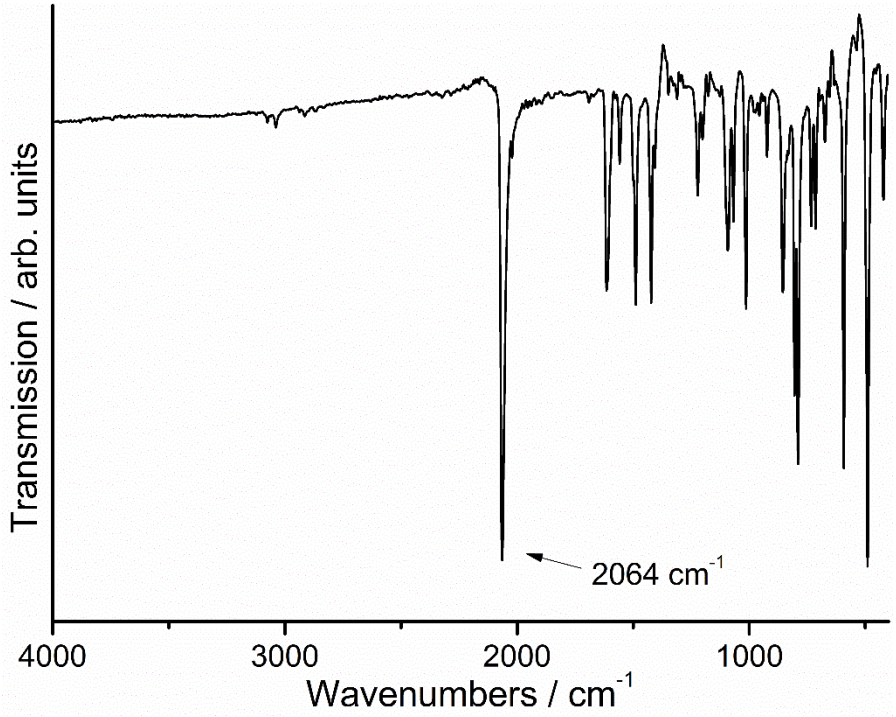

Figure S1: IR spectra of **1**. The CN stretching vibration is given.

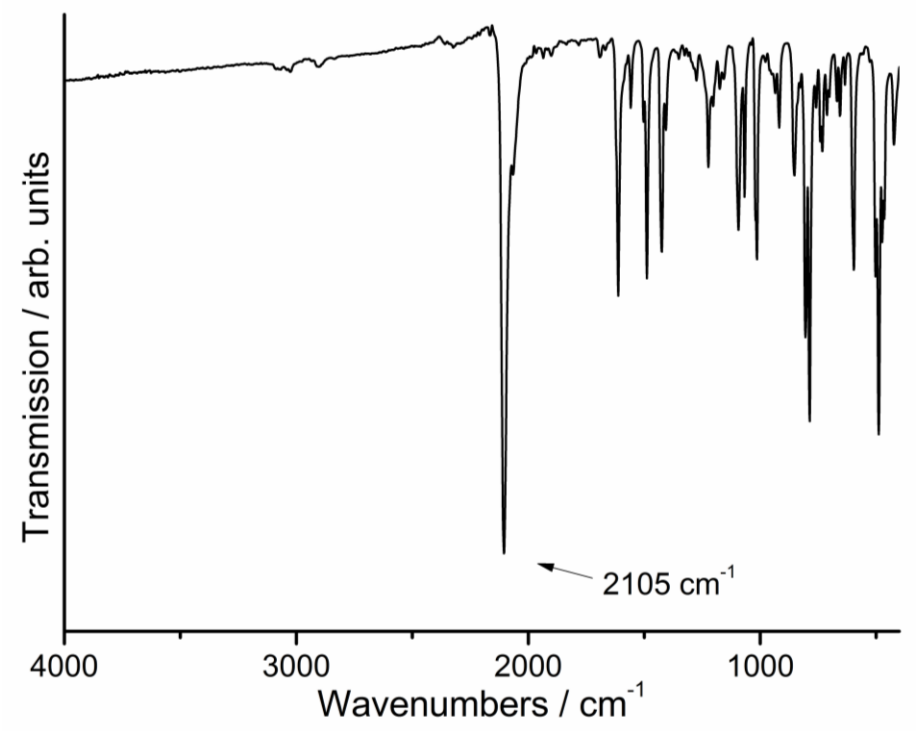

Figure S2: IR spectra of **2**. The CN stretching vibration is given.

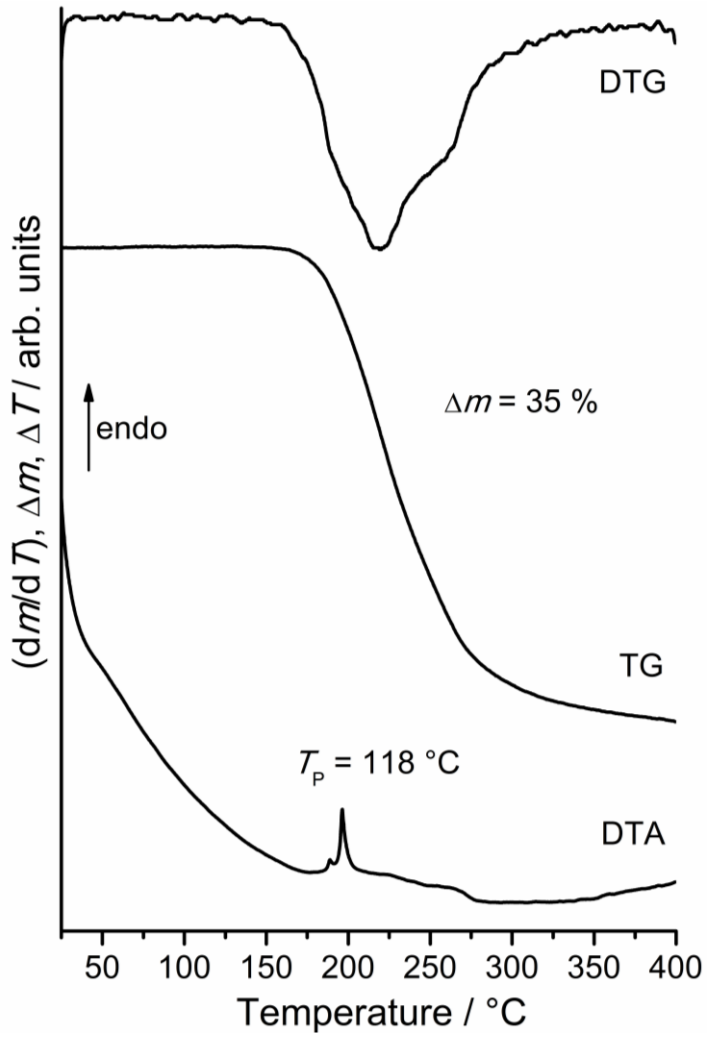

Figure S3. DTG, TG and DTA curves for **1**. Heating rate = 2 °C/min. Given are the mass change in % and the peak temperature in T_P in °C.

Table S 1: Selected bond length (Å) and angles (°) for **1**.

Co(1)-N(1)	2.0943(15)	Co(1)-N(31)	2.2412(15)
Co(1)-N(11)	2.1641(15)		
N(1)-Co(1)-N(1A)	180.00(8)	N(11)-Co(1)-N(11A)	180.00(5)
N(1)-Co(1)-N(11)	89.21(6)	N(1)-Co(1)-N(31A)	88.66(6)
N(1)-Co(1)-N(11A)	90.79(6)	N(11)-Co(1)-N(31)	90.35(6)
N(1)-Co(1)-N(31)	91.34(6)	N(11)-Co(1)-N(31A)	89.65(6)

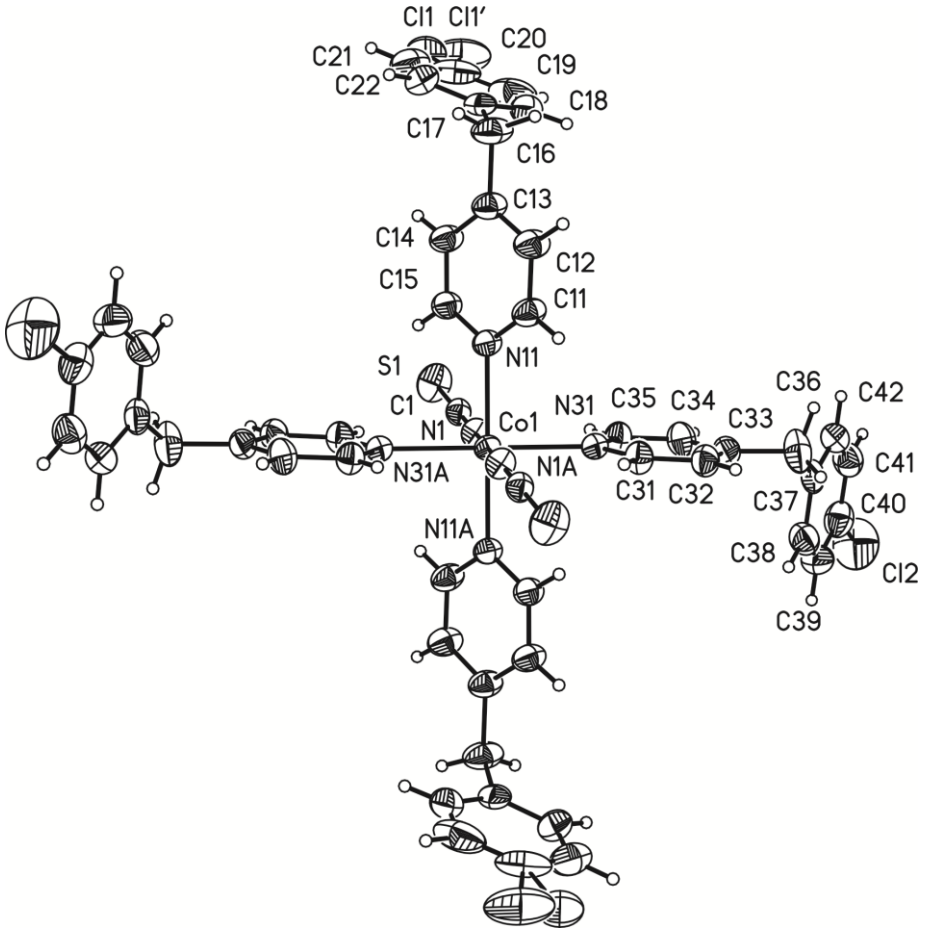

Figure S4: ORTEP plot of **1** with labelling and displacement ellipsoids drawn at 50 % probability level. Symmetry transformation used to generate equivalent atoms: A: -x+3/2,-y+1/2,-z+1.

Table S2: Selected bond length (Å) and angles (°) for **2**.

Co(1)-N(2)	2.060(2)	Co(2)-N(1A)	2.066(2)
Co(1)-S(1)	2.5694(10)	Co(2)-S(2)	2.6066(10)
Co(1)-N(11)	2.165(2)	Co(2)-N(31)	2.145(2)
N(2)-Co(1)-N(2A)	180.00(9)	N(1B)-Co(2)-N(1A)	180.00(9)
N(2)-Co(1)-N(11)	89.93(8)	N(1A)-Co(2)-N(31)	89.83(8)
N(2)-Co(1)-N(11A)	90.07(8)	N(1A)-Co(2)-N(31C)	90.17(8)
N(2)-Co(1)-S(1)	86.73(6)	N(1A)-Co(2)-S(2)	94.23(6)
N(2)-Co(1)-S(1A)	93.27(6)	N(1A)-Co(2)-S(2C)	85.77(6)

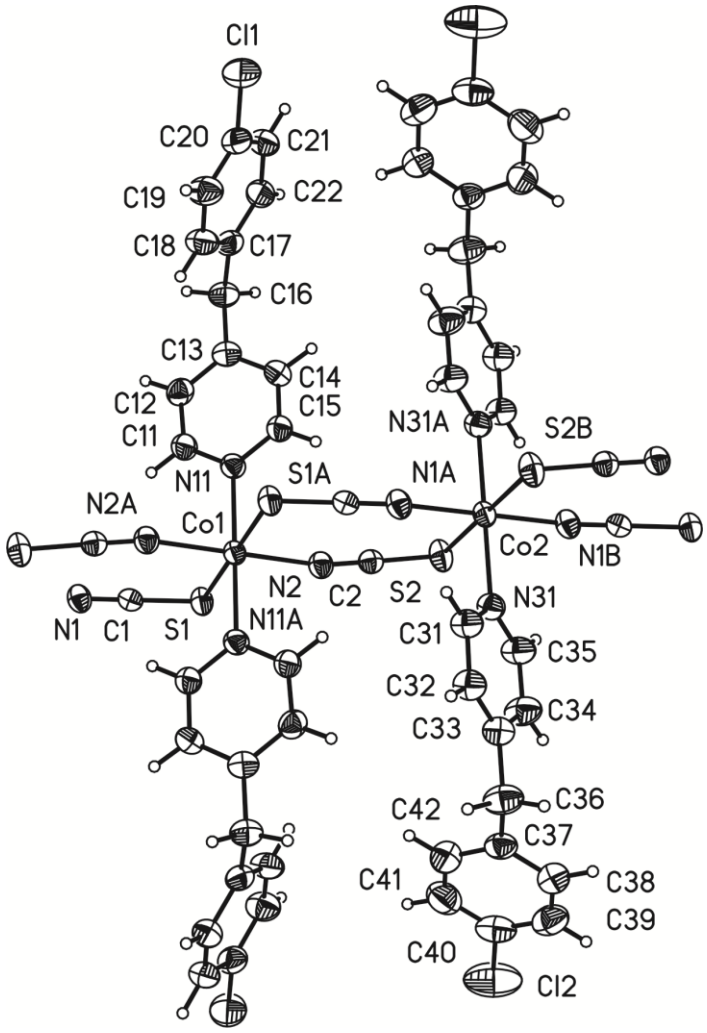

Figure S5: ORTEP plot of **2** with labelling and displacement ellipsoids drawn at 50 % probability level. Symmetry transformation used to generate equivalent atoms: A: -x+1,-y+1,-z+1, B: x-1,y+1,z, C: -x,-y+2,-z+1, D: x+1,y-1,z.

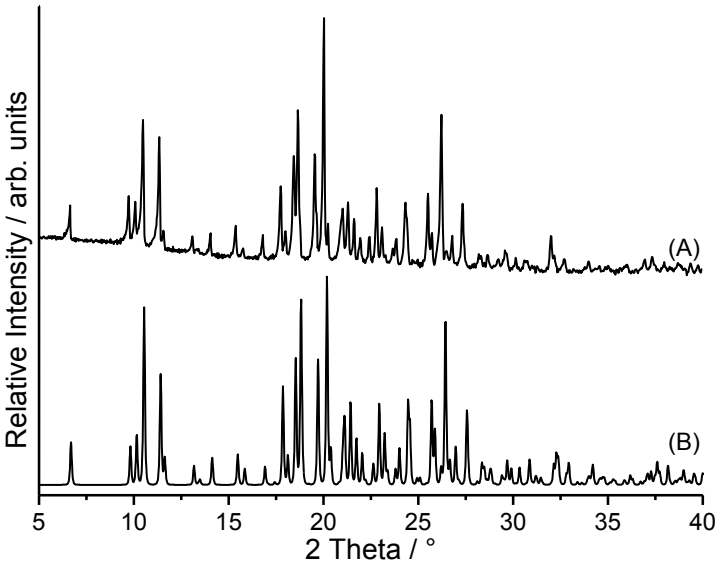

Figure S6: Experimental (top) and calculated (bottom) x-ray powder pattern for compound **1**.

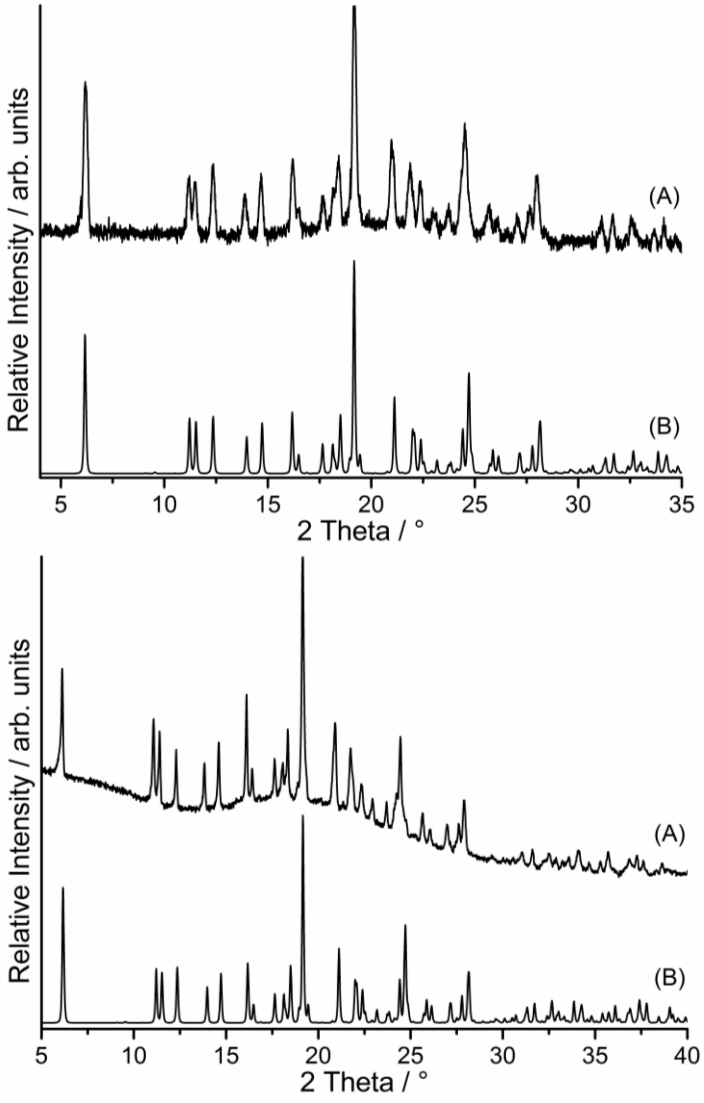

Figure S7: Experimental (top) and calculated (bottom) x-ray powder patterns for two samples of compound **2**.

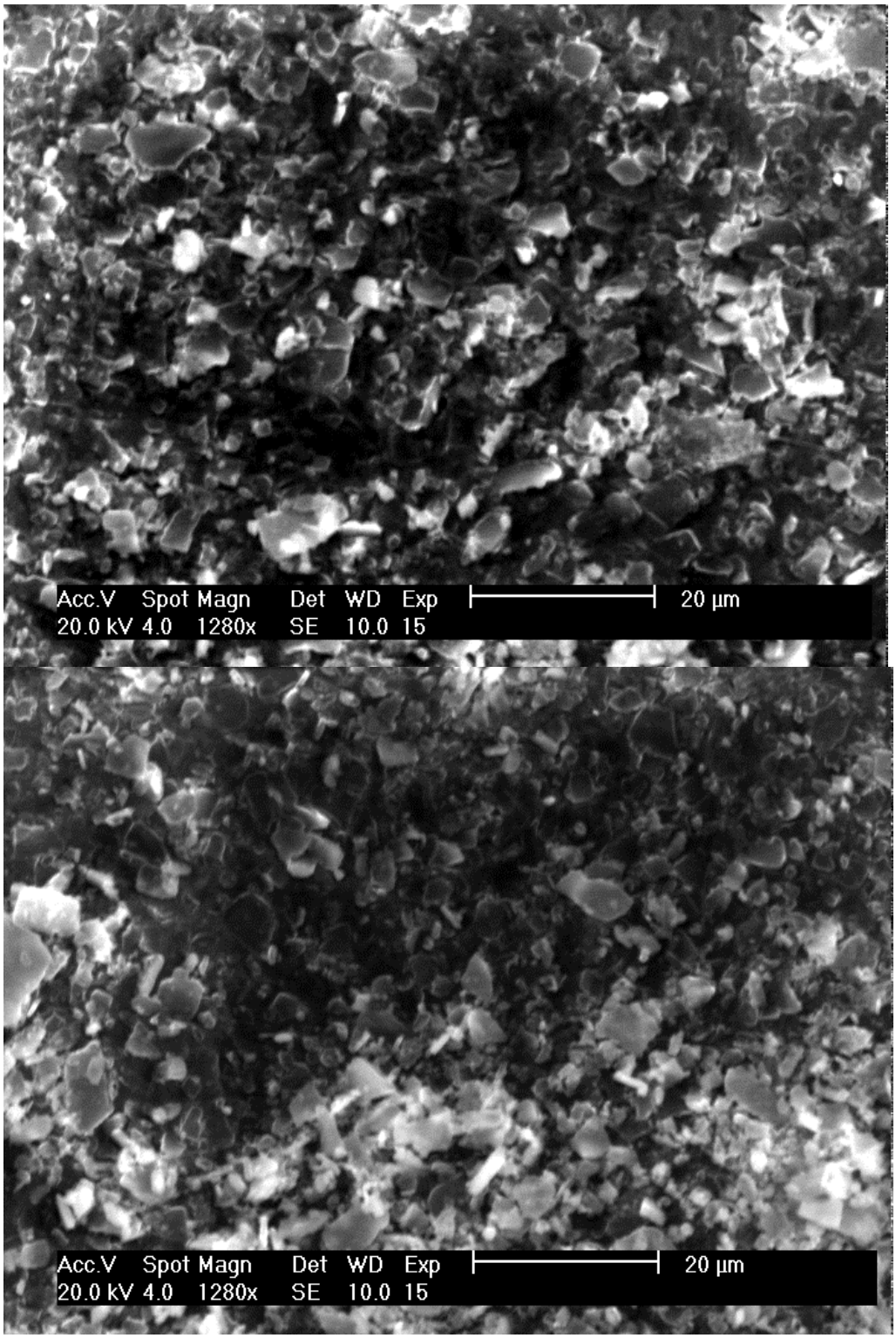

Figure S8: Selected SEM images of the crystals of compound **2**.

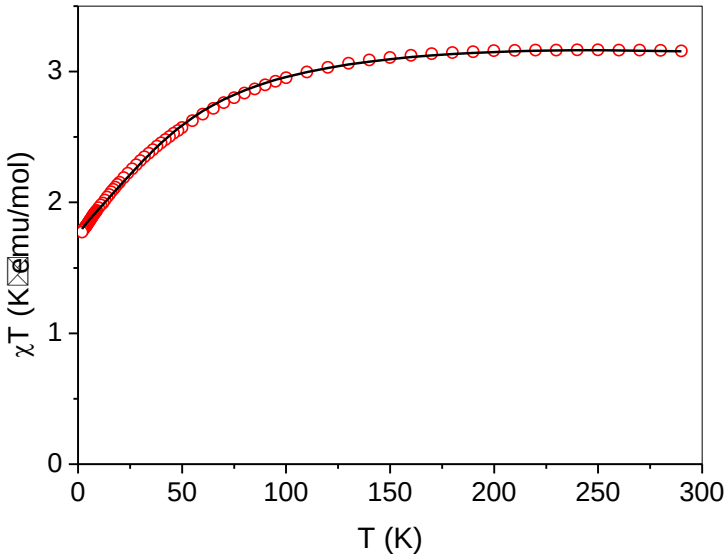

Figure S9. Temperature dependence of χ vs. *T* (top) and χ*T* vs. *T* (bottom) for **1**. The solid line is a fit done by an assumption of the axially distorted octahedral coordination of the Co(II) ion (spin orbit coupling λ=-100 ±3 cm^{-1}, orbital reduction factor κ=1.0 ± 0.02).

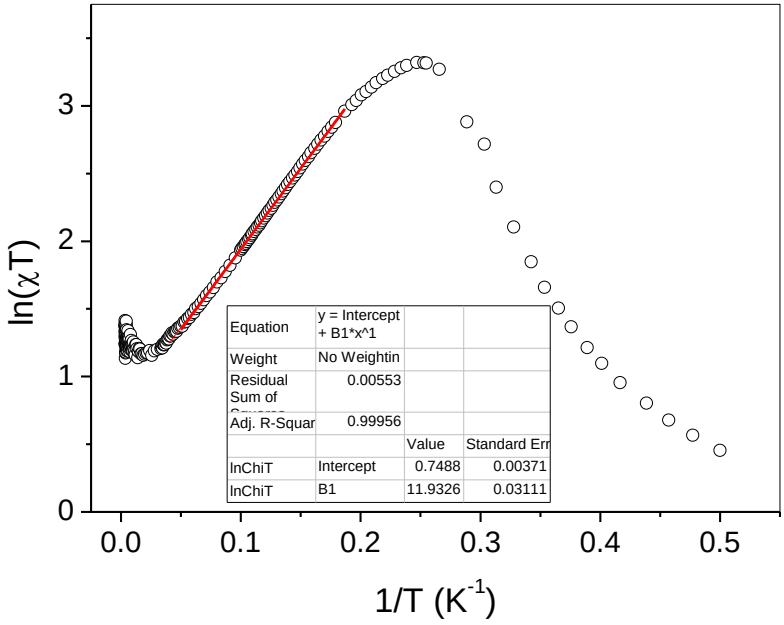

Figure S10: ln(χ*T*) vs. 1/*T* dependence for compound **2**.

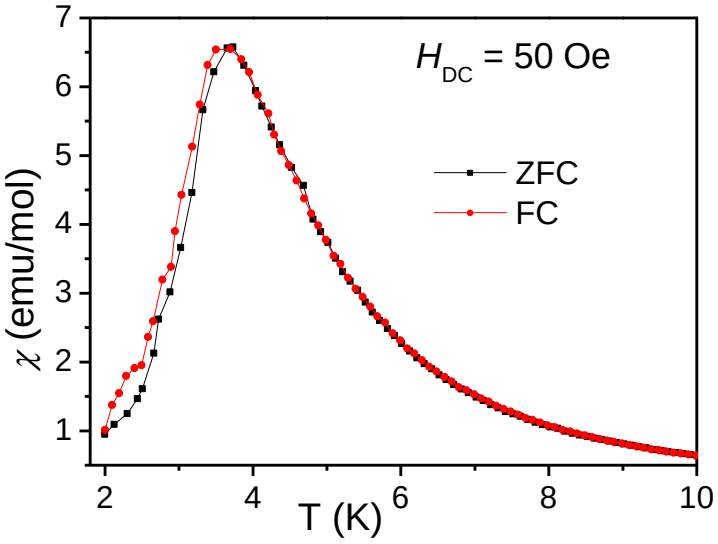

Figure S11. Comparison of $\chi(T)$ curves registered in FC and ZFC regimes for compound **2**.

Table S3: Fitting results of the AC data for compound **2**.

T (K)	χ_0	χ_∞	τ (s)	α	Reduced chi_{sqr}
3.4	4.300	0.0	5.205E-6	0.087	5.713E-4
3.3	3.590	0.0	7.102E-6	0.108	3.873E-4
3.2	2.983	0.0	9.800E-6	0.125	3.112E-4
3.1	2.484	0.0	1.405E-5	0.153	2.185E-4
3.0	2.091	0.110	2.300E-5	0.164	2.859E-4
2.9	1.753	0.129	3.581E-5	0.169	9.762E-5
2.8	1.495	0.122	5.715E-5	0.189	6.379E-5
2.7	1.296	0.109	8.516E-5	0.206	2.891E-4
2.6	1.134	0.095	1.508E-4	0.250	1.472E-4
2.5	1.007	0.104	2.868E-4	0.265	5.969E-5
2.4	0.913	0.106	5.533E-4	0.286	1.172E-5
2.3	0.821	0.112	1.02E-3	0.294	1.690E-5
2.2	0.792	0.105	2.19E-3	0.36	2.596E-5
2.1	0.770	0.110	5.28E-3	0.38	5.864E-6
2.0	0.679	0.117	8.08E-3	0.37	2.3893E-5